3-D Printed Monolithic Dielectric Waveguide Filter Using LCM Technique

Qian, Lu; Hayward, Emelia; Salek, Milan; Liu, Zhifu; Vihinen, Jorma; Wang, Yi

DOI:
10.1109/IMWS-AMP54652.2022.10106895

3-D Printed Monolithic Dielectric Waveguide Filter Using LCM Technique

Lu Qian[#], Emelia Hayward[#], Milan Salek[#], Zhifu Liu^, Jorma Vihinen*, Yi Wang[#]
[#]School of Engineering, University of Birmingham, UK
*Tampere University, Finland
^Shanghai Institute of Ceramics, Chinese Academy of Sciences, Shanghai, China
Y.Wang.1@bham.ac.uk, jorma.vihinen@tuni.fi

***Abstract*-A 3-D printed monolithic dielectric waveguide filter is presented in this paper. The proposed filter is constructed by a single piece of 3D printed dielectric puck with silver plated outer surface. To facilitate the fabrication of the monolithic dielectric filter, a lithography-based ceramic 3-D printing technology is employed. In this way, the mould required in conventional ceramic forming technologies is eliminated and the higher design freedom can be obtained. The detailed manufacturing parameters and post-processing methods are described. To demonstrate feasibility of the proposed solution, one prototype filter operating at 11.5 GHz with 850 MHz bandwidth is designed, fabricated, and measured. The measurement result shows reasonable agreement with the simulation.**

I. INTRODUCTION

Dielectric resonator filters are a class of widely employed microwave components in wireless communication systems because of their excellent performance in terms of miniature and power-handling capacity. Since the dielectric resonator was first introduced in microwave filter design, enormous advances have been achieved in the design and fabrication of the microwave dielectric filter [1], [2]. Depending on the structure and the assembly approach of dielectric resonators, dielectric filters can be categorized as two types: (i) dielectric-loaded filters, and (ii) monolithic dielectric filters. The former usually comprises dielectric pucks, mounting fixture and metallic housing. However, the extra support structures and adhesive materials may cause degradation in insertion loss and thermal stability. Monolithic dielectric filters are constructed by a dielectric puck with a metal coated surface. Compared with the dielectric loaded filter, this family of filters offers advantages in terms of the reduction in volume and weight. However, the fabrication of the filters is challenging. Special mould is often required to manufacture the dielectric puck, which is only cost-effective for large scale production and the practical design freedom is usually limited. On the other hand, binding and soldering separate dielectric blocks together requires high assembling accuracy. A minor misalignment could lead to considerable degradation in filter performance.

Additive manufacturing, also referred to as 3-D printing, has started to change the ways that microwave components are designed and fabricated. Polymer and metal-based 3-D printed microwave components have been reported [3], [4]. Advances in ceramic 3-D printing, a current trend in 3-D printing technology, have motivated researchers to apply it to microwave component design and fabrication. Some 3-D printed dielectric resonator filters were reported in [5], [6]. Manufacturing issues such as limited geometry freedom and misalignment can be alleviated to some extent. However, most of them are dielectric-loaded filter, operating in TE mode and still require custom-made metallic enclosures. Recently, 3-D printed monolithic dielectric filters operating in TM mode were reported [7], [8], where the whole filter is printed off a single piece of dielectric puck. The outer surface of the dielectric block is metallized to mimic the short-circuited contact between the dielectric resonator and metallic housing. In this way, the metallic housing can be eliminated. Compared to TM mode dielectric filters, dielectric waveguide filters can achieve further reduction of filter volume and weight. However, there is little reported work on 3-D printed dielectric waveguide filters. To fully leverage the unique free-form fabrication capability of 3-D printing and to explore the new solution for the dielectric filters, a 3-D printed monolithic dielectric waveguide filter has been designed and implemented.

In this work, the Lithography based Ceramic Manufacturing (LCM) technique [9] was used to fabricate the dielectric waveguide filter. Unlike the common stereolithography (SLA) technology, LCM is a mask-based SLA method, in which an integral image is projected to the photopolymerisable slurry surface through a special optical system. This system includes an LED light source and a digital micromirror device array. Because of the ultra-fast light switching and integral projection, LCM technology moves away from the conventional point-line-layer scanning process. Hence, the printing time can be reduced dramatically, and better feature resolution can be obtained [10].

II. MONOLITHIC DIELECTRIC WAVEGUIDE FILTER

A fourth-order dielectric waveguide filter is presented. It is centred at 11.5 GHz with a specified passband return loss of 20 dB and equal ripple bandwidth (BW) of 850 MHz. The normalized non-zero coupling coefficients m_{ij} and the external quality factor Q_{ex} are calculated to be $m_{12} = m_{34} = 0.9105$, $m_{23} = 0.6999$, $Q_{ex} = 12.68$. These design parameters can be converted to the practical filter structure by following the standard dimensioning procedure.

Fig. 1 presents the configuration of the dielectric waveguide filter, where six rectangular dielectric blocks are cascaded. The external surface of the dielectric block is fully covered by silver Two SMA connectors located on the top and bottom surfaces

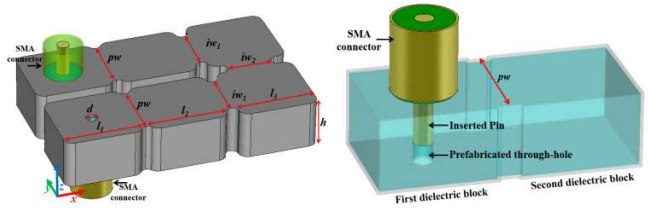

(a) (b)

Fig. 1. (a) Illustration of a fourth-order dielectric waveguide filter; (b) 3-D perspective view of the input/output coupling structure.

are input/output ports. Fig. 1(b) shows the perspective view of the feeding ports. Unlike the common feeding structures, the first dielectric block and the standard SMA connector work as the coaxial to dielectric waveguide adapter. The length of the inserted pin is fixed for ease of assembly. The external coupling strength is controlled by the width of the inductive coupling window *pw*. The TE_{101} mode in the second block is used as the first resonator. The inter-resonator coupling is realized by the inductive coupling window. Also, the round chamfer of 0.5 mm in radius is added to each upright edge of the dielectric filter model to reduce the stress accumulated at sharp corners/edges during heat treatment after printing.

Fig. 2 shows the simulated filter responses in comparison with the ideal response from the coupling matrix. As can be observed, the initial response from physical dimensioning is close to the ideal response while the response after optimization agrees well with the ideal response over the passband. The slight frequency shift and the discrepancy in out-of-band rejection are due to the higher-order spurious modes.

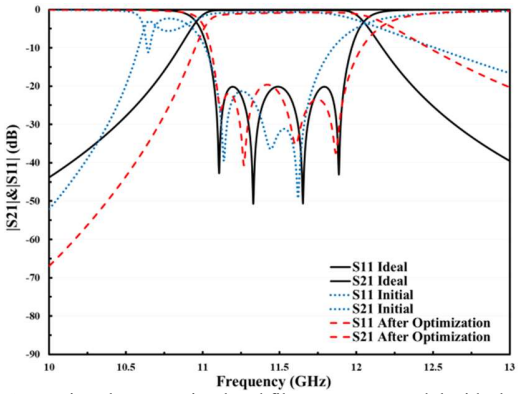

Fig. 2. Comparison between simulated filter responses and the ideal response.

III. Fabrication

A. 3-D Printing

To produce the dielectric waveguide filter, LCM technology was used. LCM is a slurry-based photopolymerization ceramic 3-D printing process. The chosen ceramic slurry is the LithaLox HP500 alumina ceramic. Its solid loading and dynamic viscosity are 49% and ~12 Pa·s at room temperature, respectively. The employed printer is the Lithoz CeraFab 7500 system. It has a maximum building envelope of 76 mm × 43 mm × 150 mm, and the nominal lateral pixel size is 40 µm. The layer thickness in printing was set to be 25 µm.

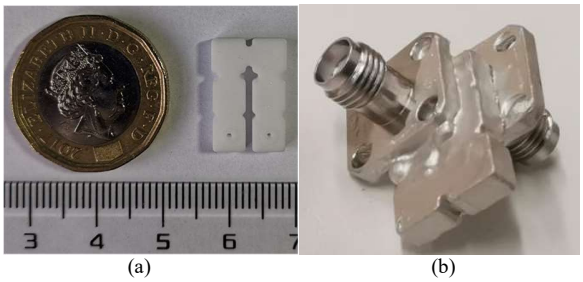

(a) (b)

Fig. 3. Photograph of the 3-D printed dielectric waveguide filter: (a) Dielectric block after sintering; (b) Dielectric waveguide filter after silver plating with assembled SMA connectors.

The manufacturing cycle can be split into two main steps: printing the green body and thermal post-processing. In the first step, the filter model was printed in a layer-by-layer fashion along the *Z*-axis (see Fig. 1(a)). No support structures are required. After printing, the green body of filter was constructed, mainly composed of weakly bound ceramic materials. Next, two thermal post-processing steps (debinding and sintering) were applied to the as-printed green body with the purpose of removing the polymer binder and achieving densification. The debinding process is the most time-consuming and critical stage since the binder and other pyrolyzed organic substances needs to be slowly removed to prevent cracking. Finally, the binder-removed sample was sintered to achieve adequate material density. The printing model needs to be scaled up to pre-compensate the shrinkage caused by thermal processes. According to previous experience, the shrinkage coefficient can be found to be 24.5% in *XY*-plane and 27.5% in *Z*-axis for the used alumina ceramic. Fig. 3(a) shows a photograph of the as-sintered dielectric puck. At this point, the dielectric component should achieve the desired electrical properties of $\varepsilon_r = 9.9$ and $\tan\delta = 0.0018$.

To evaluate the quality of the manufacture, crucial physical dimensions of the as-sintered dielectric puck (see Fig. 1(a)) were measured using the Vision Engineering Hawk inspection microscope. A comparison between the measured and designed dimensions is given in Table I. It can be found that the average dimensional variation of the dielectric puck is around 0.04~0.1 mm. This is within the manufacturing accuracy of 0.1 mm. It should be noted there are two values given for the diameter of the prefabricated through-hole, which correspond to the diameter before/after laser processing. As the prefabricated hole is smaller than the design, a laser micromachining workstation was used to expand the prefabricated holes.

TABLE I
COMPARISON BETWEEN THE MEASURED AND DESIGNED DIMENSIONS

Dimensions	Designed (mm)	Measured (mm)	Discrepancy (+/-%)
l_1	4.79	4.84	+1.0%
l_2	4.79	4.83	+0.8%
l_3	4.98	5.07	+1.8%
pw	3.84	3.80	-1.0%
iw_1	3.05	3.00	-1.6%
iw_2	2.68	2.76	+3.0%
h	3	3.10	+3.3%
d	0.8	0.73/0.94	-8.8%/+17.5%

B. *Metallization Process*

In this work, Sunchemical C2060217P3 silver paste is used to accomplish the metallization of the dielectric waveguide filter. The nominal electrical conductivity of the selected silver paste is 2.9×10^7 *S/m*. The corresponding skin depth at 11.5 GHz can be calculated to be 0.9 μm. Therefore, the thickness of the coated layer should be at least 4.5 μm (five times of the skin depth) to ensure good surface conductivity.

During the metallization process, the as-sintered dielectric block was first cleaned using acetone and deionized water in an ultra-sonic bath to remove surface contaminants. The cleaned sample was then brushed with the silver paste and was dried using a hotplate at 130 ℃ for 15 minutes. To obtain the desired coating layer thickness, the brushing and drying cycle needed to be repeated three to five times. After that, the coated sample was fired in the laboratory furnace to remove the organic solvent and binder within the silver paste and improve the adhesion between the ceramic and coating layer. The firing process was performed at 600 ℃ with a heating rate of 3 ℃/min. The sample was kept at peak temperature for 30 minutes and cooled to room temperature naturally. Fig. 3(b) shows a photograph of the dielectric waveguide filter after silver plating, where two SMA connectors were assembled using RS conductive paint 186-3600.

IV. Measurement and Discussion

The *S*-parameter measurement results and simulated filter responses are compared in Fig. 4, where the two simulated results are derived from the designed and measured physical dimensions, respectively. The inset is the expanded view of S_{21} over the passband. As can be observed, the measured filter passband is shifted down by 40 MHz (0.35% of the simulated centre frequency) against the designed response. Within the passband, the average measured insertion loss is 1.98 dB, which is 1 dB higher than the simulated result. The evident discrepancy in the insertion loss is believed to be due to the degraded effective conductivity and worse-than-simulated S_{11}. From experience, the latter observation, along with the frequency shift, is mainly caused by the dimensional inaccuracy of the manufactured prototype. To verify this point, the filter was simulated again using the measured physical dimensions in Table I. From Fig. 4, the simulated filter response based on measured dimensions shows good agreement with the measured result. The remaining difference could be attributed to assembly error, such as a gap between SMA connectors and the dielectric filter. To improve the consistency with the design, it is believed that the dimension errors can be corrected by pre-compensating the manufacture model.

V. Conclusion

A 3-D printed monolithic dielectric waveguide filter has been reported in this paper. To the best of authors' knowledge, this is the first demonstrated 3-D printed monolithic dielectric waveguide filter. The complete design and manufacturing process was illustrated. A filter prototype was fabricated using

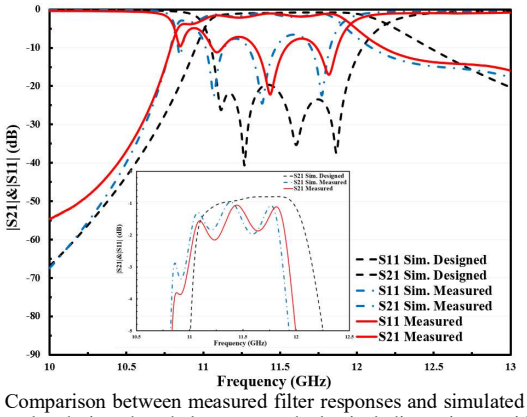

Fig. 4. Comparison between measured filter responses and simulated results based on the designed and the measured physical dimensions, with inset showing the expanded view of S_{21} over the passband

LCM ceramic 3-D printing technology. Detailed manufacturing parameters and post-processing methods were presented. The discrepancy between the measurement results and simulation results were discussed. The feasibility of manufacturing the monolithic dielectric waveguide filter using LCM technology is verified. An end-to-end manufacturing approach was demonstrated. This work opens new opportunities for the design and fabrication of dielectric resonator filters. Future work is expected to focus on improving the manufacturing accuracy through pre-compensation and implementing more complex microwave components.

References

[1] M. Memarian and R. R. Mansour, "Quad-mode and dual-mode dielectric resonator filters," *IEEE Trans. Microw. Theory Tech.*, vol. 57, no. 12, pp. 3418–3426, Dec. 2009.

[2] Y. Jang, J. Kim, S. Kim, and K. Lee, "Design and fabrication of a compact 3-dimensional stacked type dielectric ceramic waveguide bandpass filter," *IEEE Microw. Wirel. Components Lett.*, vol. 24, no. 10, pp. 665–667, 2014.

[3] C. Guo, J. Li, X. Shang, M. J. Lancaster, and J. Xu, "Progress on microwave devices fabricated using stereolithography 3-D printing technique," *2017 Int. Appl. Comput. Electromagn. Soc. Symp. China, ACES-China 2017*, no. 2, pp. 2–3, 2017.

[4] L. Qian *et al.*, "A Narrowband 3-D Printed Invar Spherical Dual-Mode Filter With High Thermal Stability for OMUXs," *IEEE Trans. Microw. Theory Tech.*, vol. 70, no. 4, pp. 2165–2173, Apr. 2022.

[5] Y. Marchives, N. Delhote, S. Verdeyme, and P. M. Iglesias, "Wide-band dielectric filter at C-band manufactured by stereolithography," *Eur. Microw. Week 2014 Connect. Futur. EuMW 2014 - Conf. Proceedings; EuMC 2014 44th Eur. Microw. Conf.*, pp. 187–190, 2014.

[6] A. Perigaud, O. Tantot, N. Delhote, S. Verdeyme, S. Bila, and D. Baillargeat, "Bandpass Filter Based on Skeleton-like Monobloc Dielectric Pucks Made by Additive Manufacturing," *2018 48th Eur. Microw. Conf. EuMC 2018*, pp. 296–299, 2018.

[7] C. Carceller, F. Gentili, D. Reichartzeder, W. Bösch, and M. Schwentenwein, "Development of monoblock TM dielectric resonator filters with additive manufacturing," *IET Microwaves, Antennas Propag.*, vol. 11, no. 14, pp. 1992–1996, 2017.

[8] D. Miek *et al.*, "Ceramic Additive Manufactured Monolithic X-Shaped TM Dual-Mode Filter," *IEEE J. Microwaves*, no. April, pp. 1–11, 2022.

[9] U. K. F. M. R. W. Homaw. Längle, "Light-curing ceramic slips for the stereolithographic preparation of high-strength ceramics," US9403726B2, 2014.

[10] Z. Chen *et al.*, "3D printing of ceramics: A review," *J. Eur. Ceram. Soc.*, vol. 39, no. 4, pp. 661–687, 2019.